Journal of Fluorine Chemistry 240 (2020) 109655

Contents lists available at ScienceDirect

Journal of Fluorine Chemistry

journal homepage: www.elsevier.com/locate/fluor

# Reductive photo-chemical separation of the hexafluorides of uranium and molybdenum

Riane E. Stene [a,b], Tobias Chemnitz [a,b], Winfried Petry [b,*], Florian Kraus [a,*]

[a] Anorganische Chemie, Phillips-Universität Marburg, Hans-Meerwein-Straße 4, 35032 Marburg, Germany

[b] Neutron Research Source Heinz Maier-Leibitz (FRM II), Technische Universität München, Lichtenbergstraße 1, 85748 Garching, Germany

ARTICLE INFO

*Keywords:*
Separation
Molybdenum
Uranium
Hexafluoride
Sulfur dioxide
Carbon monoxide
UV radiation

ABSTRACT

Two new techniques are described for the separation of molybdenum hexafluoride ($MoF_6$) from uranium hexafluoride ($UF_6$). Both separation techniques utilize the differences displayed by the hexafluorides in their ability to absorb light in the near UV region. Because $UF_6$ absorbs light in the near UV region and $MoF_6$ does not, this observation was used to selectively reduce $UF_6$ to uranium pentafluoride ($UF_5$) through irradiation with 395 nm light in the presence of a suitable reducing agent. Two reducing agents were chosen for this study: gaseous, liquid, or super-critical carbon monoxide (CO) and liquid sulfur dioxide ($SO_2$). Since $MoF_6$ is not reduced under the reaction conditions described here, it may be removed via distillation from the uranium-containing sample after complete reduction of $UF_6$ to solid $UF_5$. The molybdenum- and uranium-containing samples were measured for purity through elemental analysis using microwave plasma atomic emission spectroscopy (MP-AES). Elemental analysis showed more than 98.8 % of the Mo had been removed from the U-containing samples. Further analyses of the samples were performed by X-ray powder diffraction and IR spectroscopy.

## 1. Introduction

Currently, $^{99m}$Tc is used in over 80 % of all nuclear diagnostic techniques [1–3]. Globally, over 30 million applications of $^{99m}$Tc are utilized each year [1,2]. Today, the majority of the world's supply of $^{99m}$Tc is produced by the irradiation of uranium targets in nuclear reactors [1–4]. This irradiation process produces the isotope $^{99}$Mo, which decays with a half-life of 66 h to $^{99m}$Tc, see Eq. (1) [3].

$$^{235}\mathrm{U} \xrightarrow{(n_{\mathrm{thermal}};f)} {}^{99}\mathrm{Mo} \xrightarrow[\beta^-]{66\ \mathrm{hours}} {}^{99m}\mathrm{Tc} \qquad (1)$$

For reasons of production efficiency, typical targets for the production of $^{99}$Mo were made with highly enriched uranium (HEU, 93 % enrichment) and composed of a uranium aluminum alloy ($UAl_x$). However, the current political consensus requests that the usage of HEU for civilian purposes be substituted by low enriched uranium (LEU, enrichment 19.75 %) wherever technically and economically feasible [5,6]. As part of this consensus, the affected irradiation facilities and target-production facilities have spent the past several years implementing changes that will allow for the production and irradiation of LEU targets for $^{99}$Mo fabrication. However, the yield of $^{99}$Mo per irradiation cycle, depending on the irradiation facility and target used, is expected to decrease by at least a factor of two [7]. The decreased yield of $^{99}$Mo per target is a direct effect of the lower $^{235}$U content. Consequently, a larger number of targets will need to be irradiated in order to meet the worldwide demand of $^{99}$Mo.

After irradiation of a target at a nuclear facility, the target is sent to a nearby processing facility. At these facilities, a wet-chemical process is used to extract and purify $^{99}$Mo. During extraction, the entire target – including the aluminum cladding – is dissolved in an alkaline solution containing either NaOH or KOH [8]. After this initial dissolution and extraction procedure, the dissolved molybdenum can be further purified by passing the solution through a series of anion/cation exchange and aluminum oxide columns, and then by sublimation [9].

Because the extraction and purification of $^{99}$Mo relies on a wet-chemical process, and because a larger number of targets will need to be irradiated to meet the worldwide demand for $^{99}$Mo, more liquid radioactive waste will be produced during the extraction and purification processes. In regard to radioactive waste production, Lee and coworkers predict that the production of 10,000 6-day Ci/week using LEU targets will lead to the production of 15,000 L of intermediate level wastes per year (and after cementation this volume is expected to increase to 375,000 L) [10]. This increase in intermediate level wastes

---

* Corresponding authors.
*E-mail addresses:* winfried.petry@frm2.tum.de (W. Petry), florian.kraus@chemie.uni-marburg.de (F. Kraus).

https://doi.org/10.1016/j.jfluchem.2020.109655
Received 11 September 2020; Received in revised form 30 September 2020; Accepted 30 September 2020

translates to a 200 % increase in radioactive waste production [10].

It is clear from these alarming numbers that new approaches for the production, extraction and purification of $^{99}$Mo from uranium should be considered in order to decrease the amount of nuclear waste produced from this industry. Recently, our group has developed a cylindrical LEU target consisting of a uranium foil encapsulated between two coaxial aluminum cladding cylinders, which can be mechanically de-cladded before target processing [11]. This design allows separate processing of the irradiated target and cladding material during the first steps of the $^{99}$Mo extraction process [11]. Since this target may be mechanically de-cladded, and allows for processing of the pure irradiated foil, different approaches to processing the bare uranium foil may also be realized, such as fluorinating the foil to obtain mixtures of uranium hexafluoride ($UF_6$) and molybdenum hexafluoride ($MoF_6$) (along with other potentially volatile fission product fluorides).

It has previously been suggested that $UF_6$ gas streams can be purified from contaminants using ultraviolet light and a fluorine radical scavenger [12–14]. In the purification technique described by Fields, $UF_6$ was purified from $MoF_6$ using UV light having "sufficient energy to photodissociate $MoF_6$ and $UF_6$" to $MoF_5$ and $UF_5$ (an exact wavelength of 254 nm was used). Fields argues that uranium can be purified from molybdenum using this process because $UF_5$ is more reactive than $MoF_5$ and will, consequently, further react with fluorine radicals/unreacted molecules of $MoF_6$ to regenerate $UF_6$. However, no data concerning the purity or the yields of either the $UF_6$ or $MoF_5$ samples is reported in this work. Because the separation technique described by Fields is hard to control and is indiscriminate towards the reduction of $UF_6$ and $MoF_6$, it was suspected that this method would be unsuitable for the separation of $MoF_6$ from $UF_6$, with the purpose of extracting and purifying $MoF_6$. Experiments in our laboratory have confirmed this opinion.

Two new techniques for the separation of $MoF_6$ from $UF_6$, both with natural isotope distribution, using reducing agents and near ultraviolet radiation having a wavelength of 395 nm, are described in this work. Two reducing agents were studied, namely, carbon monoxide (CO, gaseous, liquid and supercritical) and sulfur dioxide ($SO_2$, liquid). Future research will need to show whether or not the reactions can be transferred to the separation of $^{99}MoF_6$ from $UF_6$ after a target has been irradiated in a nuclear reactor.

## 2. Results and discussion

### 2.1. Selection of a suitable wavelength of UV light

It has long been known that the hexafluorides of U and Mo can be reduced using UV light and a reducing agent, such as CO, $SO_2$, or $H_2$ [15, 16]. Using CO as an example, Eqs. (2) and (3) illustrate these reduction reactions.

$$2UF_6 + CO \xrightarrow{\text{UV light of sufficient energy}} 2UF_5 + COF_2 \tag{2}$$

$$2MoF_6 + CO \xrightarrow{\text{UV light of sufficient energy}} 2MoF_5 + COF_2 \tag{3}$$

For these reactions to occur under ambient conditions, careful selection of the wavelength of UV light needs to be considered. If the UV light chosen does not have sufficient energy to excite the hexafluoride, then selective photochemical reduction will not occur. It can be seen from the UV absorption spectrum of $UF_6$ that weak absorption occurs between 360–400 nm, whereas strong absorption begins around 340 nm and continues into the far UV range [17]. In the UV absorption spectrum of $MoF_6$, absorption begins at about 280 nm and extends into the far UV range [18].

Using these observations, we could demonstrate that $MoF_6$ could be selectively removed from $UF_6$ by careful selection of the wavelength of UV light. That is, if UV light having a wavelength longer than about 300 nm is used, $UF_6$ can be selectively reduced to $UF_5$ while $MoF_6$ remains unaffected. Since both known modifications of $UF_5$ are non-volatile solids and $MoF_6$ is a highly volatile liquid at room temperature (b.p. 34 °C), this technique could be used to separate $MoF_6$ from $UF_6$. In the present work, a wavelength of 395 nm was chosen for these selective reduction reactions. Using CO as an example, the separation process is given by Eqs. (4) and (5).

$$2UF_6 + CO \xrightarrow{395\text{ nm}} 2UF_5 + COF_2 \tag{4}$$

$$2MoF_6 + CO \xrightarrow{395\text{ nm}} \text{No reaction} \tag{5}$$

### 2.2. Separation of $MoF_6$ from $UF_6$ using gaseous carbon monoxide and near UV light

The separation of $MoF_6$ from $UF_6$ is described by Eqs. (4) and (5). To perform this separation, 200 mg of $UF_6$ and 200 mg of $MoF_6$ were condensed at −196 °C (using liquid nitrogen) into an approximately 30 mL quartz reaction vessel. The hexafluorides were allowed to warm to room temperature to ensure adequate mixing. After warming, the mixture was cooled to −196 °C and the vessel was pressurized with 1 bar of CO. The vessel was allowed to warm to room temperature and then irradiated with near ultraviolet light having a wavelength of 395 nm for about 24 h. After this time, a blue-green product was observed ($UF_5$, see Fig. 1). The reaction mixture was cooled to −196 °C, the excess CO and $COF_2$ product were pumped off, and then 1 bar of fresh CO was added to the vessel. The reaction mixture was irradiated once more with 395 nm light for an additional 24 h. During these irradiation cycles, $UF_6$ was selectively reduced to $UF_5$ while $MoF_6$ remained unreacted. The reduction of $UF_6$ was considered to be complete after visual indication that the $UF_5$ formed turned from blue-green to pale green. After complete reduction of $UF_6$ to $UF_5$, the reaction mixture was cooled once more to −196 °C and the remaining CO and $COF_2$ were pumped off. Once all CO and $COF_2$ had been pumped away, the reaction vessel was warmed to room temperature and the $MoF_6$ was removed from the solid $UF_5$ sample by distillation into a new quartz vessel using liquid nitrogen cooling. Fig. 1 depicts the laboratory set-up for this separation technique. Fig. S1 provides a step-by-step schematic of the separation.

Quantitative yields of $UF_5$ and $MoF_6$ were obtained after separation. This separation technique was repeated three times to establish reproducibility. The separate $UF_5$ and $MoF_6$ samples were then tested for purity through elemental analysis with microwave plasma atomic emission spectroscopy (MP-AES). For easier analysis and sample preparation, the $MoF_6$ sample obtained after this separation procedure was further reduced to $MoF_5$ using CO as a reducing agent and UV light having a wavelength of 254 nm (Eq. (6) and Fig. 2).

$$2MoF_6 + CO \xrightarrow{252\text{ nm}} 2MoF_5 + COF_2 \tag{6}$$

The results of the elemental analyses of the $UF_5$ samples obtained after each separation are given in Table 1. Each sample was measured in triplicate (Trial 1 (U) – Trial 3 (U)); more information regarding the analysis of these samples is given in the Material and Methods Section. Although some amount of molybdenum was present in these samples, over 99 % of the original molybdenum content was removed using the separation technique described here. The percentages of uranium observed in these samples are also given in Table 1. A pure sample of $UF_5$ should contain about 71.48 % U, however, the samples analyzed here contained 68.61–73.52% U. This difference in percentages is due to hydrolysis of the $UF_5$ samples during sample preparation and dissolution for MP-AES measurement, see Materials and Methods Section.

To further characterize the $UF_5$ sample obtained after the CO separation procedure described here, an X-ray powder diffraction pattern was obtained, of which a Rietveld refinement is shown in Fig. 3. This powder pattern agrees nicely with previously published data for β-$UF_5$ (Fig. S3) [20], but one peak due to an unidentified phase appeared at ca. 31.85° 2θ. Details of the Rietveld refinement are reported in Table S1. Therefore, β-$UF_5$ is essentially obtained as a pure phase, however some

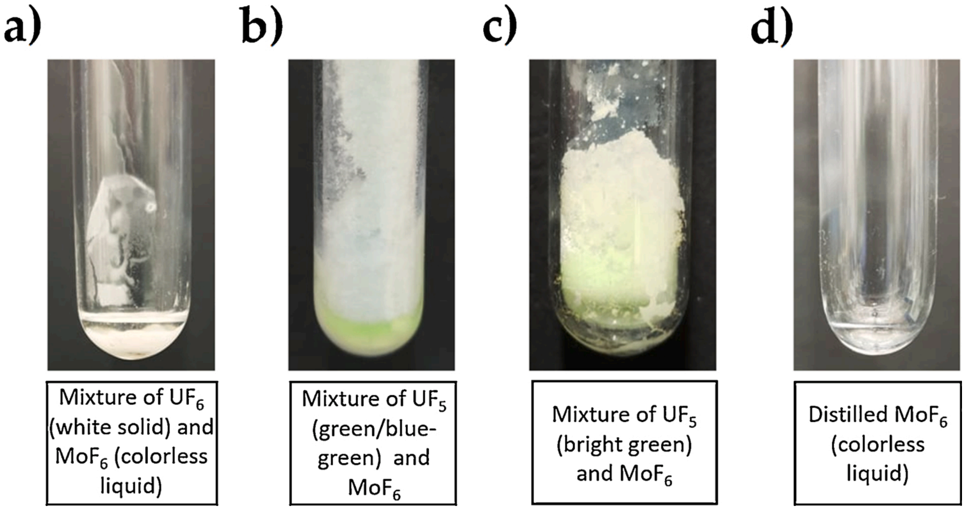

**Fig. 1.** Laboratory set-up for the separation of $MoF_6$ from $UF_6$ using CO and near UV light. **a)** Mixture of $MoF_6$ (colorless liquid), $UF_6$ (white solid) and CO (colorless gas) at room temperature. **b)** Reaction mixture after 24 h of irradiation with 395 nm light. Blue-green $UF_5$ has formed, $MoF_6$ has not been reduced. **c)** Reaction mixture after the second irradiation cycle (24 h). A mixture of pale green $UF_5$ and $MoF_6$ is obtained. **d)** The unreacted $MoF_6$ was removed from the solid $UF_5$ by distilling the hexafluoride into a new quartz vessel. ***Note:*** There is no/very little $UF_6$ present in the $MoF_6$ sample because no solid, white $UF_6$ is visible.

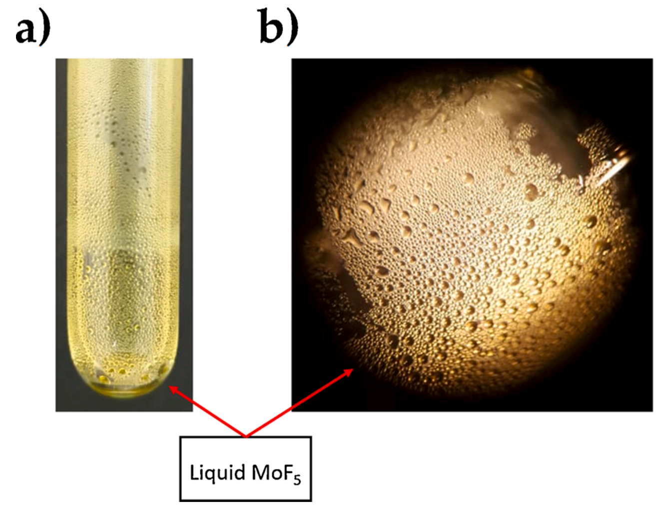

**Fig. 2.** Yellow $MoF_5$ obtained after the reduction of the $MoF_6$ sample. **a)** The bulk sample inside a quartz tube. **b)** A section of the sample as seen under a microscope. No visual traces of pale green $UF_5$ can be seen in this sample, which speaks towards the purity of the Mo sample and quality of the separation. ***Note:*** $MoF_5$ can readily be obtained as a supercooled liquid at room temperature [19].

**Table 1**
MP-AES results of the uranium sample ($UF_5$) obtained after the near UV separation of $MoF_6$ from $UF_6$ using 395 nm light and gaseous carbon monoxide as a reducing agent. All trials were done in triplicate.

| | Trial 1 (U) | Trial 2 (U) | Trial 3 (U) |
|---|---|---|---|
| Mo, mg/L | 0.16 ± 0.01 | 0.16 ± 0.01 | 0.13 ± 0.00 |
| % Mo | 0.30 ± 0.01 | 0.32 ± 0.01 | 0.26 ± 0.00 |
| U, mg/L | 39.31 ± 2.27 | 35.62 ± 0.77 | 35.52 ± 0.95 |
| % U | 73.52 ± 1.41 | 68.61 ± 1.70 | 68.89 ± 1.05 |
| Mo/U molar ratio before separation | 1.70 | 1.63 | 1.61 |
| Mo/U molar ratio after separation | 0.01 ± 0.00 | 0.01 ± 0.00 | 0.01 ± 0.00 |
| % Mo removed | 99.41 ± 0.02 | 99.30 ± 0.03 | 99.42 ± 0.01 |

amorphous impurities may be present as indicated by the bump in the background, which is also due to the glass capillary used for the measurement.

Additionally, an IR spectrum in the region from 400 to 4000 $cm^{-1}$ was recorded for the $UF_5$ sample obtained after the separation (Fig. 4). This IR spectrum agrees nicely with previously reported IR spectra for β-$UF_5$ [21]; slight evidence of beginning hydrolysis is present.

The elemental analyses results for the $MoF_5$ samples, obtained by the reduction of $MoF_6$, are given in Table 2. Due to the oily nature of the $MoF_5$ sample, the entire sample was dissolved in distilled water and then diluted for elemental analysis; Trial 1 (Mo) – Trial 3 (Mo) were obtained from the same separation batches as those stemming from the U determinations reported in Table 1. More information regarding the analysis of these samples is given in the Material and Methods section. It can be seen from Table 2 that no uranium was detected in these samples. The detection limit for U on the device used to measure the samples was approximately 0.5 mg/L, which correlates with a U impurity of less than three percent. However, since no visual evidence of uranium as white $UF_6$ or green $UF_5$ was seen in the $MoF_6$ or $MoF_5$ samples, the purity of these samples is thought to be greater than 97 %. Additionally, the percentages of Mo in the samples are given in Table 2. A sample containing pure $MoF_5$ should contain 50.26 % Mo, however, the samples measured in this work have Mo contents ranging from 36.34 to 40.02 %. These lower percentages are a direct consequence of the hydrolysis of the $MoF_5$ samples (by releasing HF to produce molybdenum oxides or oxyfluorides) during sample preparation for MP-AES measurement.

In order to further characterize the molybdenum sample collected after the CO separation described here, a fourth separation was performed. The $MoF_6$ collected was reduced to $MoF_5$ using the reaction described by Eq. (6). An oil of $MoF_5$ was obtained that was allowed to crystallize under inert atmosphere in a glovebox over the course of about a week. After crystallization, an X-ray powder diffraction pattern of the sample was obtained. The powder pattern matched that of previously reported powder patterns of $MoF_5$ (Fig. S4) [22]. The powder pattern and the Rietveld refinement are shown in Fig. 5. Further details of the Rietveld refinement are reported in Table S2, and showed $MoF_5$ was obtained phase-pure.

Additionally, an IR spectrum of the $MoF_5$ sample was obtained. This IR spectrum matches nicely with previously reported IR spectra of $MoF_5$ [19,22,23], although very slight hydrolysis is obviously present, Fig. 6.

### *2.3. Separation of $MoF_6$ from $UF_6$ using sulfur dioxide and near UV light*

Similar to the gaseous CO separation, $MoF_6$ can be removed from $UF_6$ using near UV light and $SO_2$ as a reductant. During this separation, $UF_6$ is selectively reduced to $UF_5$ through interaction with the 395 nm light and the $SO_2$ solvent (Eq. (7)). $MoF_6$ remains unaffected by the near UV light, but does slowly react with $SO_2$ to form $MoOF_4$ (Eq. (8)). However,

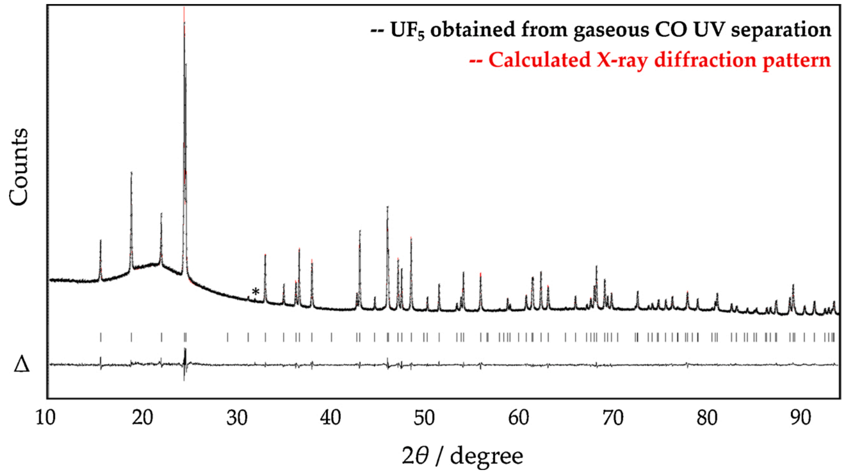

**Fig. 3.** Observed and calculated powder X-ray pattern of β-$UF_5$ after Rietveld refinement. The calculated reflection positions are indicated by the vertical bars below the pattern. The curve at the bottom represents the difference (Δ) between the observed and the calculated intensities. $R_p = 2.01$, w$R_p = 2.71$ (not background corrected $R$ values), $S = 1.71$. The asterisk indicates the foreign peak.

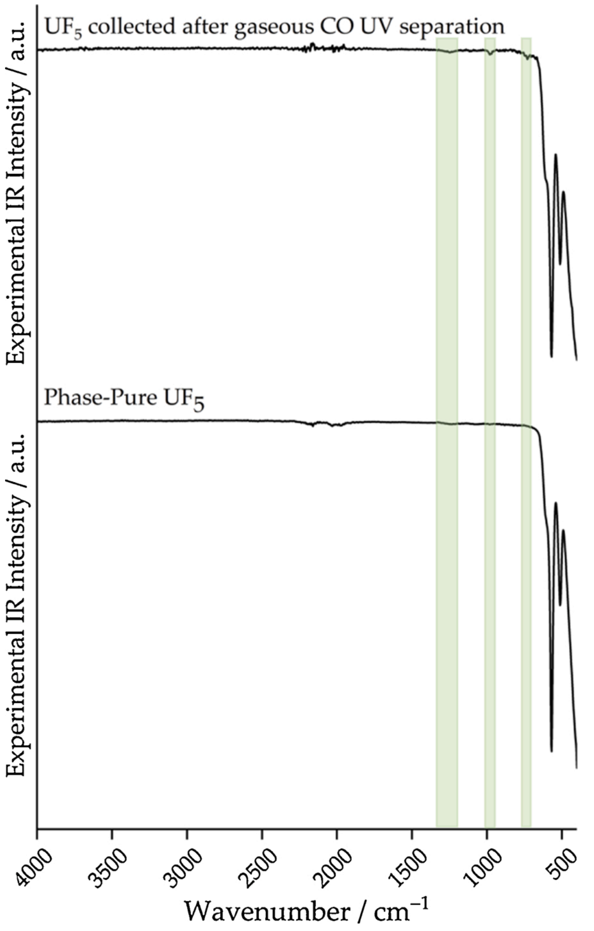

**Fig. 4.** IR spectrum of the $UF_5$ sample obtained after the separation of $MoF_6$ from $UF_5$ using gaseous CO and near UV light. The above spectrum agrees with previously reported spectra for β-$UF_5$. The light-green overlays indicate very weak bands arising from slight hydrolysis of the sample that occurred during sample handling. The noise around 2000 cm$^{-1}$ is due to the diamond ATR-IR.

**Table 2**

MP-AES results of the molybdenum sample obtained after the UV separation of $MoF_6$ from $UF_6$ using 395 nm light and gaseous CO as a reducing agent. A single sample was prepared for each trial.

| | Trial 1 (Mo) | Trial 2 (Mo) | Trial 3 (Mo) |
|---|---|---|---|
| Mo, mg/L | 29.14 | 26.29 | 28.95 |
| % Mo | 39.99 | 36.34 | 40.02 |
| U, mg/L | n.d. | n.d. | n.d. |

n.d. = not detected.

the reaction of $MoF_6$ with $SO_2$ is so slow that it plays no role during the time frame of the separation procedure.

$$2UF_6 + SO_2 \xrightarrow[\text{very fast}]{395\ \text{nm}} 2UF_5 + SO_2F_2 \tag{7}$$

$$MoF_6 + SO_2 \xrightarrow[\text{very slow}]{} MoOF_4 + SOF_2 \tag{8}$$

In this separation, 200 mg of $UF_6$ and 200 mg of $MoF_6$ were condensed at −196 °C into an FEP reaction vessel (containing a 1 cm Teflon-coated stir bar). About six grams of $SO_2$ were condensed onto the hexafluoride mixture. The mixture was allowed to warm to room temperature and the solution was stirred using a stir plate (note: the reaction vessel must be able to withstand the vapor pressure of the liquid $SO_2$ at room temperature). Once the hexafluorides were completely dissolved in the $SO_2$ solution, the $UF_6/MoF_6/SO_2$ mixture was irradiated under constant stirring with 395 nm light for 1 h and 30 min. During irradiation, $UF_6$ was selectively reduced to $UF_5$ while $MoF_6$ remained unreacted and soluble in the $SO_2$ solution, whereas $UF_5$ is insoluble in $SO_2$ and precipitated from solution. After irradiation, a solution of $MoF_6$ dissolved in $SO_2$ was obtained along with precipitated $UF_5$ sitting at the bottom of the reaction vessel. The $MoF_6/SO_2$ reaction mixture was then distilled to a new FEP reaction vessel using liquid nitrogen cooling. The molybdenum-containing sample was extracted from the $SO_2$ solution after one week as white, crystalline $MoOF_4$ (Eq. (8)). Fig. 7 depicts the laboratory set-up for this separation technique. Fig. S2 provides a step-by-step schematic for the separation.

After separation, quantitative yields of $UF_5$ were obtained, however, yields of only about 60–70 % were obtained for the $MoOF_4$ samples. These decreased yields can result from a variety of reasons. Most likely, the $MoF_6$ had not completely reacted with the $SO_2$ solution after a week of reaction time. Longer reaction time is probably needed for full conversion of $MoF_6$ to $MoOF_4$. Another reason that the yields were relatively low is due to the fact that $MoF_6$ is soluble in the FEP plastic used

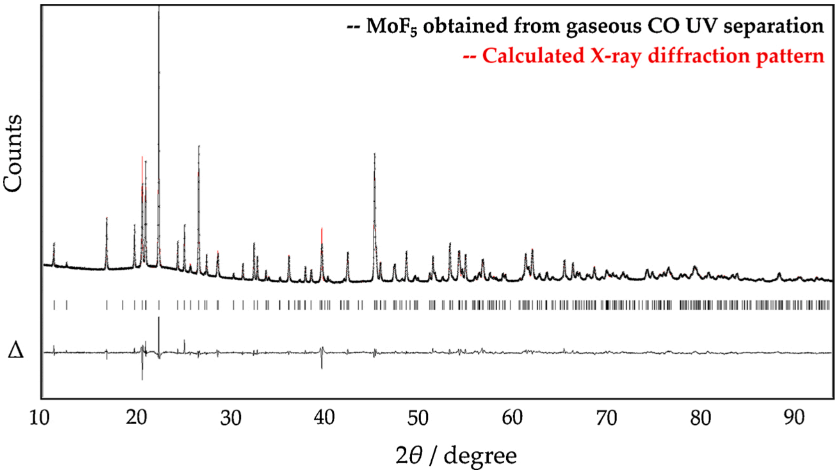

**Fig. 5.** Observed and calculated powder X-ray pattern of MoF$_5$ after Rietveld refinement. The calculated reflection positions are indicated by the vertical bars below the pattern. The curve at the bottom represents the difference (Δ) between the observed and the calculated intensities. $R_p = 3.25$, w$R_p = 4.73$ (not background corrected $R$ values), $S = 3.63$.

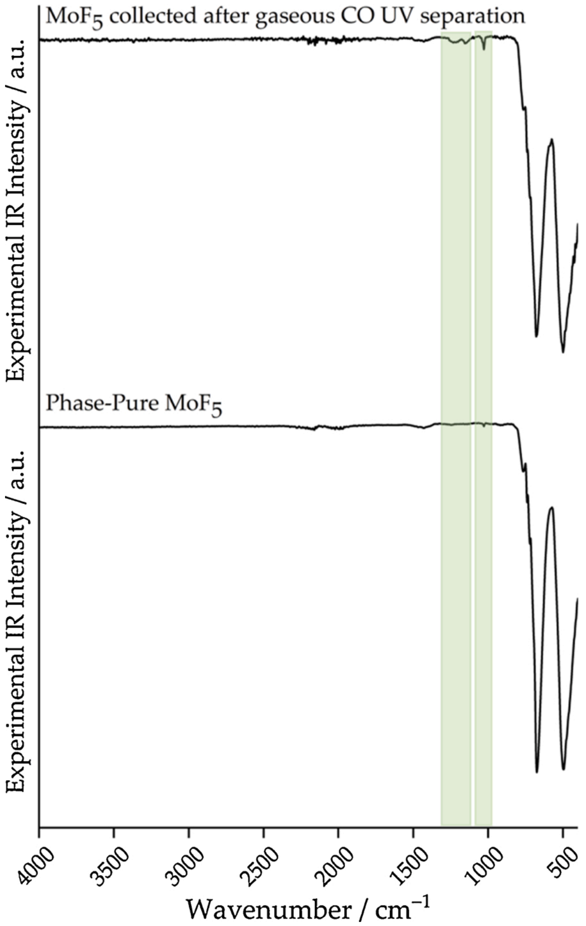

**Fig. 6. Top:** IR spectrum of the MoF$_5$ obtained after the separation of MoF$_6$ from UF$_6$ using CO and near UV light. The MoF$_6$ was further reduced to MoF$_5$ using gaseous CO and 254 nm light. **Bottom:** IR spectrum of pure MoF$_5$. The light-green overlays indicate bands arising from slight hydrolysis of the sample that occurred during sample handling. The noise around 2000 cm$^{-1}$ is due to the diamond ATR-IR.

for the reaction vessels. It is suggested that glass or quartz vessels be used for future applications of this separation technique in order to increase the yield of the molybdenum-containing sample. Alternatively, it should be possible to extract all the Mo by passing the MoF$_6$/SO$_2$ solution through an aqueous solution of NaOH or KOH, however, the influence of the formed SO$_3^{2-}$ anion then needs to be investigated. Since the purpose of this work was to provide techniques for non-aqueous separations, the aqueous extraction of Mo from SO$_2$ was not tested. Although such a dissolution process is foreseeable, the primary goal of the $^{99}$Mo industry is making $^{99}$Mo/$^{99m}$Tc available to the physicians and patients in a soluble form, preferably MoO$_4^{2-}$. Moreover, to test the reproducibility of this separation technique, the separation was repeated in triplicate. Afterwards, the separate UF$_5$ and MoOF$_4$ samples were tested for purity by elemental analyses with MP-AES.

The results of the elemental analyses of the UF$_5$ samples obtained after each separation are given in Table 3. Each sample was measured in triplicate (Trial 4 (U) – Trail 6 (U)); more information regarding the analyses of these samples is given in the Material and Methods section. While some amount of molybdenum was present in these samples, over 98.8 % of the original molybdenum content was removed using the separation technique described here. The percentage of uranium observed in these samples is also given in Table 3. As previously stated, a pure sample of UF$_5$ should contain about 71.48 % U, however, the samples analyzed here contained between 62.82–73.01% U. This difference in percentages is due to hydrolysis of the UF$_5$ samples during sample preparation. Additionally, it is suspected that some sulfur-containing species are present in these samples, as discussed below.

To further characterize the UF$_5$ samples collected after the SO$_2$ separations, an X-ray powder diffraction pattern was obtained. This powder pattern was very similar to the pattern observed for the UF$_5$ samples obtained after the CO separations reported here (Fig. S5) and agrees with previously reported patterns for β-UF$_5$ [20], however, evidence for a small amount of an unidentified crystalline impurity is present. The results of a Rietveld refinement performed on this X-ray powder diffraction pattern is provided in Fig. 8 and Table S3.

Additionally, IR spectra of the UF$_5$ samples, obtained in the region from 400 to 4000 cm$^{-1}$, showed some impurities were present in these samples (Fig. 9). In the work of Halstead and coworkers, where the synthesis of UF$_5$ is discussed, the authors acknowledge that UF$_5$ can be synthesized by reduction of UF$_6$ with SO$_2$, but with product purities less than those obtained with CO reductions [15]. To exclude the possibility of these foreign IR bands arising from molybdenum-containing species, the experiment described here was repeated, but only with UF$_6$, that is, no MoF$_6$ was added. The IR spectrum obtained from the reduction of UF$_6$ with SO$_2$ and 395 nm light looks nearly identical to the spectra obtained for the UF$_5$ samples collected after the SO$_2$ separations; Fig. 9 shows a comparison. Therefore, it was concluded that these foreign bands arise

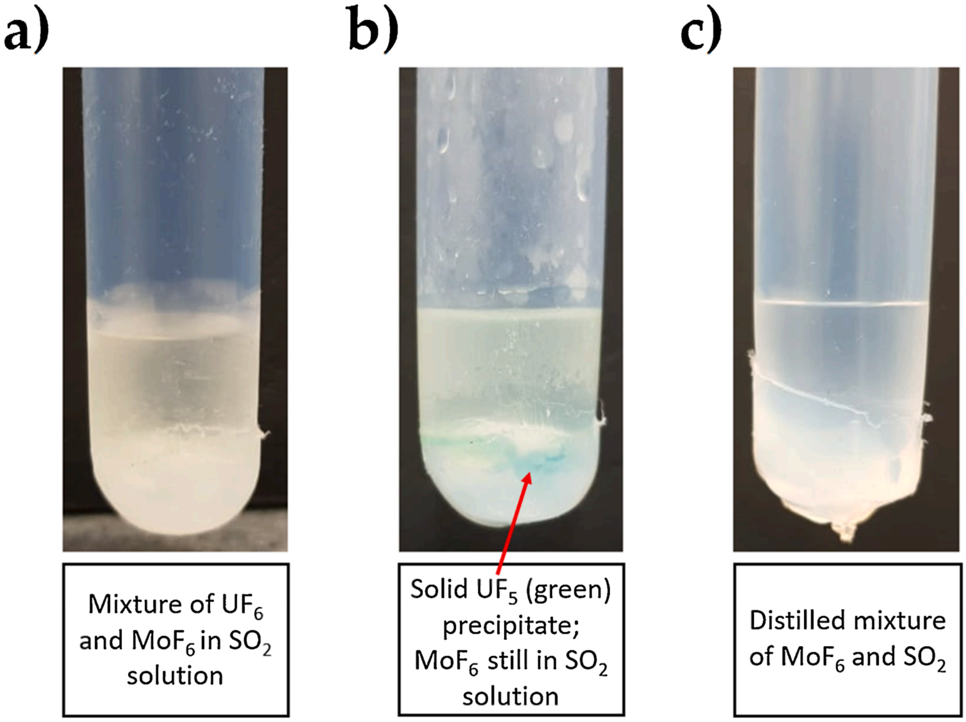

**Fig. 7.** Laboratory set-up for the separation of $MoF_6$ from $UF_6$ using $SO_2$ and near UV light. **a)** $UF_6$ and $MoF_6$ dissolved in an $SO_2$ solution. ***Note:*** Solutions of $UF_6$ in $SO_2$ are slightly yellow. **b)** The solution after irradiation with 395 nm light. Pale green $UF_5$ has formed and has precipitated from the $SO_2$ solution while $MoF_6$ remains unreacted and dissolved in $SO_2$. **c)** The $MoF_6/SO_2$ solution is removed from the solid $UF_5$ via distillation. ***Note:*** This solution is colorless, indicating that little or no $UF_6$ is present in this solution.

**Table 3**
MP-AES results of the uranium sample ($UF_5$) obtained after the $SO_2$/UV separation of $MoF_6$ from $UF_6$ using 395 nm light and $SO_2$ as a solvent. All trials were measured in triplicates.

| | Trial 4 (U) | Trial 5 (U) | Trial 6 (U) |
|---|---|---|---|
| mg Mo / L | 0.08 ± 0.00 | 0.28 ± 0.03 | 0.10 ± 0.01 |
| % Mo | 0.15 ± 0.01 | 0.50 ± 0.02 | 0.17 ± 0.00 |
| mg U / L | 37.44 ± 0.25 | 34.78 ± 2.54 | 36.22 ± 3.77 |
| % U | 73.01 ± 2.35 | 62.82 ± 0.42 | 63.11 ± 0.43 |
| Mo/U molar ratio before separation | 1.64 | 1.68 | 1.65 |
| Mo/U molar ratio after separation | 0.01 ± 0.00 | 0.02 ± 0.00 | 0.01 ± 0.00 |
| % Mo removed | 99.69 ± 0.02 | 98.81 ± 0.04 | 99.58 ± 0.01 |

as intrinsic impurities in the synthesis of $UF_5$ by reduction of $UF_6$ in $SO_2$ and not from molybdenum-containing species. Unfortunately, the identity of the impurities could not be determined, although it is suspected that they are sulfur-containing compounds.

The results of the elemental analyses of the $MoOF_4$ samples are given in Table 4. Each sample was measured in triplicate. Trial 4 (Mo) – Trial 6 (Mo) were obtained from the same separation batches as those stemming from the U determinations reported in Table 3. More information regarding the analyses of these samples is given in the Material and Methods section. It can be seen from Table 4 that no uranium was detected in these samples. As previously discussed, the detection limit for U on the device used to measure the samples was approximately 0.5 mg/L, which correlates to a U impurity of less than 1.5 % in these samples. However, because there was no visual evidence of uranium (as pale green $UF_5$) present in the white $MoOF_4$ sample, the purities of these samples are thought to be greater than 98.5 %. Additionally, the

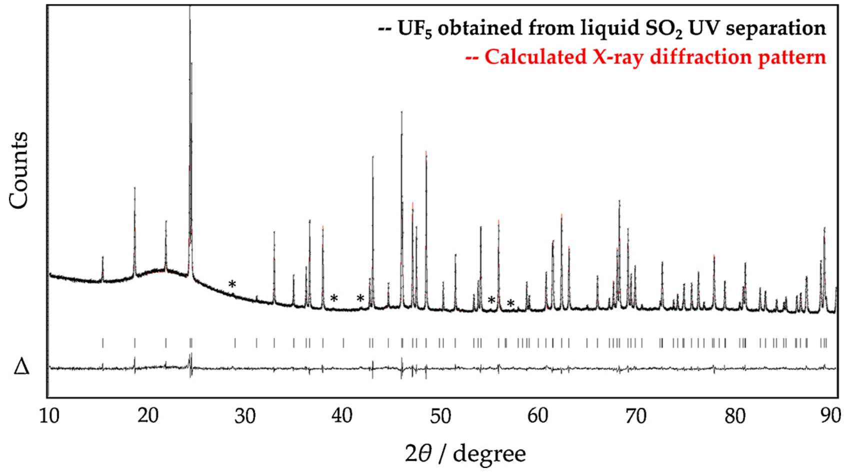

**Fig. 8.** Observed and calculated powder X-ray pattern of β-$UF_5$ after Rietveld refinement. The calculated reflection positions are indicated by the vertical bars below the pattern. The curve at the bottom represents the difference (Δ) between the observed and the calculated intensities. $R_p = 2.14$, $wR_p = 2.83$ (not background corrected $R$ values), $S = 1.69$. The asterisks indicate foreign peaks.

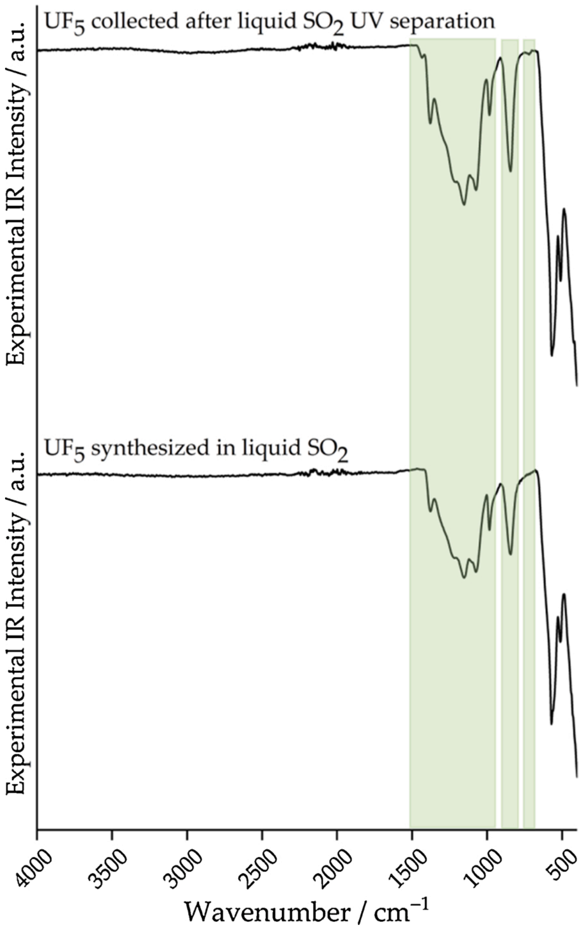

**Fig. 9.** **Top)** IR spectrum of a $UF_5$ sample obtained after the separation of $MoF_6$ from $UF_5$ using $SO_2$ and near UV light. **Bottom)** IR spectrum of a $UF_5$ sample obtained after the reduction of $UF_6$ with $SO_2$ and near UV light (in the absence of $MoF_6$). The light-green overlays indicate bands arising from impurities intrinsic to the synthesis of $UF_5$ in $SO_2$ solution. These impurities are likely sulfur-containing species. The noise around 2000 cm$^{-1}$ is due to the diamond ATR-IR.

**Table 4**
MP-AES results of the molybdenum sample ($MoOF_4$) obtained after the $SO_2$/UV separation of $MoF_6$ from $UF_6$ using 395 nm light and $SO_2$ as a solvent. All trials were measured in triplicate.

| | Trial 4 (Mo) | Trial 5 (Mo) | Trial 6 (Mo) |
|---|---|---|---|
| Mo, mg/L | 54.24 ± 2.55 | 55.90 ± 3.71 | 55.92 ± 1.11 |
| % Mo | 54.65 ± 1.23 | 50.59 ± 1.33 | 49.96 ± 0.83 |
| U, mg/L | n.d. | n.d. | n.d. |

n.d. = not detected.

percentages of Mo present in the samples are given in Table 4. A sample containing pure $MoOF_4$ should contain 51.05 % Mo, however, the samples measured in this work have Mo contents between 49.96–54.65% Mo. The differences in these percentages in comparison with the theoretical value are a direct consequence of some hydrolysis that occurred during sample preparation.

To further characterize the $MoOF_4$ sample obtained after the $SO_2$ separation procedure described here, an X-ray powder diffraction pattern was obtained. This powder pattern agrees with previously obtained patterns of $MoOF_4$ measured in our laboratory although the crystallinity of both samples is quite low [24]. A comparison of the powder pattern obtained here with a previously obtained pattern is provided in Fig. S6. The results of a Rietveld refinement performed on this X-ray powder diffraction pattern is reported in Fig. 10 and Table S4 and suggests that $MoOF_4$ has been obtained phase-pure, however the presence of amorphous impurities cannot be excluded.

Additionally, an IR spectrum of the $MoOF_4$ obtained in this study was collected in the region 400–4000 cm$^{-1}$. A comparison with a previous IR spectrum of pure $MoOF_4$ synthesized in our laboratory is provided in Fig. 11.This IR spectrum shows the presence of $MoOF_4$ along with some hydrolysis species or perhaps some sulfur-containing impurities [24].

### *2.4. Separation of $MoF_6$ from $UF_6$ using liquid CO or supercritical CO and near UV light*

In the work described here, a typical separation of $MoF_6$ from $MoF_6$/$UF_6$ mixtures using gaseous CO and near UV light took about two days, whereas the same separation with $SO_2$ took an hour and 30 min. The shorter reaction time needed for the $SO_2$ separation is most likely a consequence of the higher concentration of liquid reducing agent in comparison with the gaseous CO experiment. It was then a question of curiosity if shorter reaction times (i.e. quicker separations) could be achieved if the separation of $MoF_6$ from $UF_6$ was performed using supercritical CO or liquid CO and near UV light. The results from these experiments will be briefly discussed.

Because CO has a critical pressure of 34.98 bar, all experiments using its supercritical state were performed in a suitable high-pressure container. This container was made from stainless steel AISI 316 L and equipped with a 5 mm thick sapphire window as well as a liquid nitrogen-cooled cold finger. Additionally, this vessel was connected to a storage cylinder that contained supercritical CO. A mixture consisting of roughly 17 mg $MoF_6$ and 42 mg $UF_6$ was condensed into this high-pressure container by cooling the cold finger. The exact masses of each hexafluoride are given in the Materials and Methods section. Subsequently, 8.7 mmol CO having a pressure of 56 bar was added to the reaction vessel. The high-pressure container was allowed to warm to room temperature and then irradiated with near ultraviolet light at a wavelength of 395 nm for 60 min, whereupon the temperature rose to ca. 33 °C. During the course of the reaction, the formation of filaments of a light-blue solid were observed, originating from the cold finger. These became denser over time until finally covering the entire sapphire window. Analysis of these filaments using X-ray powder diffraction suggest this light-blue solid to be β-$UF_5$. The course of the reaction is shown in Fig. 12.

The highly-volatile portion of the reaction products from the first trial was evaluated using gas phase IR spectroscopy, Fig. 13. As expected, the IR spectrum showed the presence of unreacted CO as well as $COF_2$ [25]. In addition, it also showed the presence of oxalyl fluoride $(COF)_2$ [26], and traces of $MoF_6$ [27,28].

For analysis of separation efficiency, the high-pressure container was allowed to warm to room temperature and the volatile components were distilled into a separate FEP vessel at liquid nitrogen temperature. Because both CO and $COF_2$ possess significant vapor pressures, even at −196 °C, they could be subsequently evaporated [29–32]. The remaining volatile components, namely $MoF_6$ and unreacted $UF_6$, were dissolved and analyzed for Mo and U content using MP-AES. The non-volatile solid remaining in the high-pressure container, mostly $UF_5$, was dissolved in dilute $HNO_3$ and also analyzed for Mo and U content by MP-AES. Additional information on the collection of MP-AES data as well as the IR spectrum are given in the Material and Methods section. Table 5 shows the original composition of the $UF_6$/$MoF_6$ mixture as well as the composition of the respective samples after separation. The amount of Mo found in the high-pressure container amounts to about 1 % of the original amount, highlighting the observation that $MoF_6$ is not affected by the irradiation at 395 nm, even under high-pressure reducing atmospheres. The amount of uranium found in the volatile section can be attributed to unreacted $UF_6$. The sapphire window is slowly covered with a layer of $UF_5$ during the separation procedure, which likely blocks a considerable amount of radiation, thereby preventing a complete

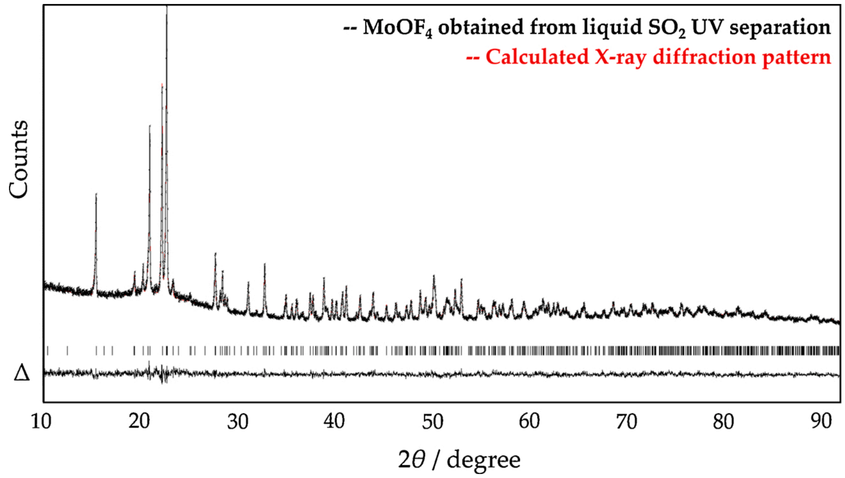

**Fig. 10.** Observed and calculated powder X-ray pattern of β-UF$_5$ after Rietveld refinement. The calculated reflection positions are indicated by the vertical bars below the pattern. The curve at the bottom represents the difference (Δ) between the observed and the calculated intensities. $R_p = 3.93$, $wR_p = 4.99$ (not background corrected $R$ values), $S = 1.46$.

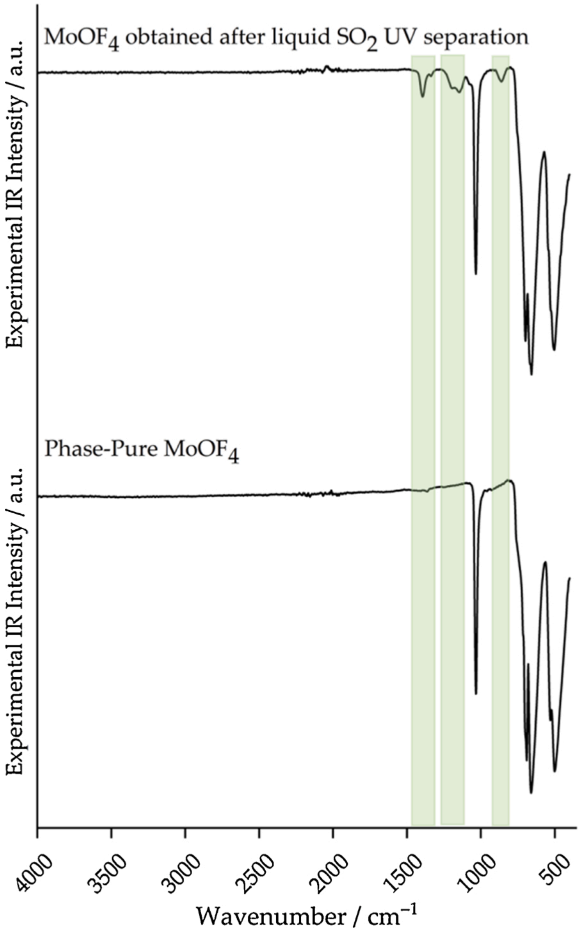

**Fig. 11. Top)** IR spectrum of a MoOF$_4$ sample obtained from the SO$_2$ separation procedure. **Bottom)** Previously measured IR spectrum of MoOF$_4$ obtained in our laboratory. The light-green overlays indicate bands arising from slight hydrolysis of the sample that occurred during sample handling. The noise around 2000 cm$^{-1}$ is due to the diamond ATR-IR.

reduction UF$_6$ to UF$_5$. This circumstance may be countered by an optimized design of the high-pressure container.

In order to investigate the separation using liquid CO, a mixture consisting of 18 mg MoF$_6$ and 36 mg UF$_6$ was condensed into an FEP cold trap at −196 °C using liquid nitrogen. Dried CO was carefully condensed onto the hexafluorides, ensuring complete coverage, and the cold trap subsequently taken away. Irradiation was performed for 30 min at 395 nm. The apparatus was cooled during the entire irradiation period to −196 °C. After irradiation, the volatile species were pumped off with continuous liquid nitrogen cooling and the cold trap was then allowed to warm to room temperature. Optical inspection did not reveal any signs of residues such as UF$_5$. Subsequent analysis of the remaining volatile species was performed using gas phase IR spectroscopy (Fig. 14).

The evaluation of the IR spectra of the mixture prior to and after separation yields the masses listed in Table 6.

The results of the two trials are not entirely consistent. For both trials, the major amount of UF$_6$ could be recovered and remained unreacted. However, the first trial showed traces of COF$_2$ after the separation in addition to the bands of CO in the IR spectrum, indicating some amount of reduction of UF$_6$. The second trial also shows bands belonging to CO, however, the bands belonging to COF$_2$ are absent. This observation is in accordance with a significantly lower recovery of UF$_6$ for the first trial, whereas the recovered amount of MoF$_6$ is identical for both trials. Further investigations are required to resolve this contradiction. Nevertheless, it may be stated that the reaction rate with liquid CO is significantly reduced with respect to supercritical CO due to the low temperature.

### 2.5. *Brief comments on the reactivities of fluorides under discussion*

In the separation of UF$_6$ from MoF$_6$ described by Fields, it is stated that UF$_6$ may be separated from MoF$_6$ on the basis of the reactivities of their corresponding pentafluorides [14]. Fields argues that UF$_5$ is more reactive than MoF$_5$. Therefore, by reducing both MoF$_6$ and UF$_6$ to their corresponding pentafluorides, UF$_5$ may react further with any excess MoF$_6$ and fluorine radicals to reproduce UF$_6$, thus allowing for its separation from solid MoF$_5$. However, as is evident from the work described here, UF$_5$ does not react with MoF$_6$ under the conditions used in the present study.

Considering the crystal structures of UF$_5$ and MoF$_5$, the most reactive, volatile, and soluble pentafluoride should be MoF$_5$, because its solid-state structure consists of isolated Mo$_4$F$_{20}$ molecules [22,33]. UF$_5$, on the other hand, has two polymorphs – α-UF$_5$ (high-temperature modification) and β-UF$_5$ (low-temperature modification). It is anticipated that α-UF$_5$ will be more reactive, volatile and soluble than β-UF$_5$ because its solid-state structure consists of one-dimensional, infinite

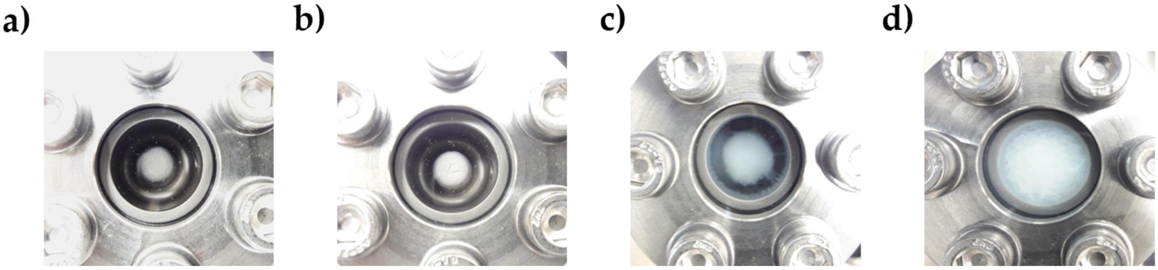

**Fig. 12.** View into the high-pressure container through the sapphire window. From left to right: **a)** Mixture of $UF_6$ and $MoF_6$ condensed on the cold finger. **b)** After venting the chamber with supercritical CO. **c)** After irradiation for 7 min. **d)** The end of irradiation after 60 min.

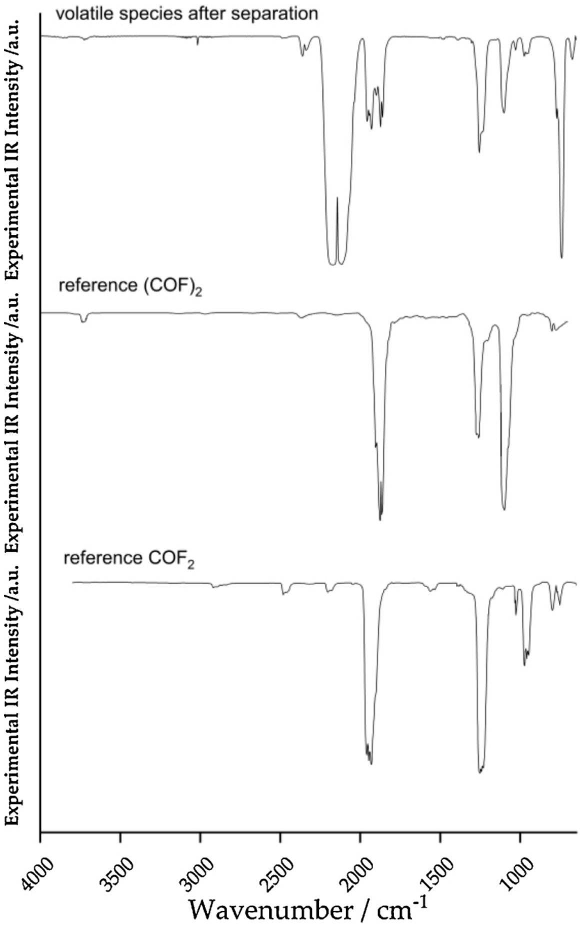

**Fig. 13. Top)** IR spectrum of the volatile section of the reaction products containing CO, $(COF)_2$ and $COF_2$. **Middle)** Reference IR spectrum of $(COF)_2$ [26]. **Bottom)** Reference spectrum of $COF_2$ [25].

strands of corner-sharing octahedra [34]. However, in the work described here, only β-$UF_5$ is formed, as evidenced by powder X-ray diffraction. Consequently, β-$UF_5$ should be less reactive than both α-$UF_5$ and $MoF_5$ because its solid-state structure consists of a three-dimensional, infinite network [35]. This supports the observation described in this work that $UF_5$ does not react with $MoF_6$ to produce $MoF_5$ and $UF_6$.

Because Fields does not discuss reaction yields, or give any elemental analysis, it is hard to compare the quality of his separation reactions with those described here. As discussed in the introduction, our laboratory has failed to reproduce the separations published by Fields.

**Table 5**

MP-AES results of the non-volatile contents remaining in the high-pressure container (U side), and the volatile component collected in a separate FEP vessel (Mo side) after the second supercritical CO separation trial. U and Mo masses prior to separation were determined from the IR spectrum.

| | high-pressure container (U side) | volatile section (Mo side) |
|---|---|---|
| mg Mo | 0.08 ± 0.06 | 7.35 ± 0.06 |
| at% Mo | 1.06 ± 0.8 | 98.00 ± 4.01 |
| mg U | 20.96 ± 0.63 | 2.99 ± 0.60 |
| at% U | 78.20 ± 2.51 | 11.16 ± 2.24 |
| Mo/U molar ratio before separation | 0.69 ± 0.03 | |
| Mo/U ratio after separation | 6.10 ± 1.22 | 0.009 ± 0.007 |
| at% Mo removed | 98.93 ± 0.8 | – |

## 3. Conclusions

Two separation techniques for the extraction and purification of $MoF_6$ from $UF_6$ have been described in this study. Both separation techniques utilize differences in the reactivities of the hexafluorides under irradiation with near UV light in the presence of reducing agents. $UF_6$ absorbs light in the near UV region, whereas $MoF_6$ does not. Using this difference, $UF_6$ was selectively reduced in the presence of either gaseous or supercritical CO or liquid $SO_2$ to solid $UF_5$, while $MoF_6$ did not react. After complete reduction of $UF_6$ to $UF_5$, the volatile $MoF_6$-containing sample could be separated by distillation. In most cases, over 99 % of the Mo was removed from the U-containing sample.

These separation techniques provide fast and effective methods for the extraction and purification of natural Mo from natural U. Because these techniques do not rely on sample dissolution in aqueous solutions, the separations could be achieved with minimum amounts of liquid waste production. However, future work on this project must determine if radiolysis plays any role in these separation techniques when an irradiated U target containing $^{99}Mo$ is used, and whether other fission product fluorides participate in or interfere with the reactions described here.

Since the gaseous CO separation described here lead to quantitative yields of high-purity $MoF_6$ samples, it is envisioned that this separation procedure may also be suitable for transfer to industry. The chemistry and techniques described here were performed at the laboratory scale, but this separation procedure should easily translate to larger-scale operations. In fact, if large enough sample containers, more than two to three equivalents of CO, and multiple or more powerful LED lights having a 395 nm wavelength were used, then it is anticipated that this separation technique could, in fact, be performed within a day. However, the kinetics of the process must be investigated in the future. In addition, before transfer to the $^{99}Mo$ industry can be realized, effects due to high radioactivity must be thoroughly studied.

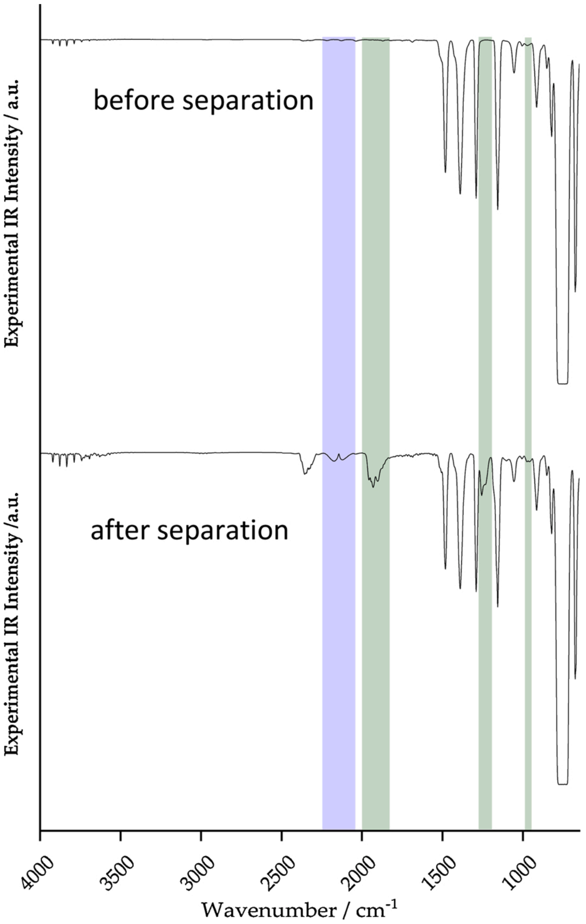

**Fig. 14. Top)** IR spectrum of the mixture in trial 1 prior to separation. **Bottom)** IR spectrum of the mixture after separation. The light-green overlay indicates the bands belonging to $COF_2$, whereas the light-blue overlay indicates the bands belonging to CO.

**Table 6**

Masses of $MoF_6$ and $UF_6$ calculated from IR spectra prior to and after irradiation.

| | Trial 1 | Trial 2 |
|---|---|---|
| $MoF_6$ initial, mg | 18.9 ± 0.1 | 17.7 ± 0.1 |
| $MoF_6$ final, mg | 16.0 ± 0.1 | 15.0 ± 0.1 |
| Mo ratio (after / before) [%] | 84.7 ± 0.7 | 84.7 ± 0.7 |
| $UF_6$ initial, mg | 37.0 ± 0.1 | 35.3 ± 0.1 |
| $UF_6$ final, mg | 31.1 ± 0.1 | 32.9 ± 0.1 |
| U molar (after / before) [%] | 84.1 ± 0.9 | 93.2 ± 1.1 |

## 4. Material and methods

### 4.1. General procedures and materials

All operations were performed in either stainless steel (316 L) or Monel metal vacuum lines, which were passivated with undiluted fluorine at various pressures before use. Preparations were carried out in an atmosphere of dry and purified Argon (5.0, Praxair). Molybdenum hexafluoride (99 %, abcr) was distilled once prior to use. Uranium hexafluoride (99 %, homemade) was distilled once prior to use. Homemade quartz reaction vessels were used for the CO separations. Fluorinated ethylene propylene, FEP, vessels were used for the $SO_2$ separations.

### 4.2. Techniques and procedures for the separation of $MoF_6$ from $UF_6$ using carbon monoxide and near UV light

Because all trials performed to demonstrate this separation technique are similar to each other, only Trial 1 will be discussed in detail here. For Trial 2 – Trial 3 and Trial 7 (performed to obtain analyses on the $MoF_5$ samples), only the amounts of starting material, yields, and sample used for MP-AES analysis will be discussed.

***Trial 1:*** A 30 mL, homemade quartz reaction vessel was attached to a glass-to-metal adaptor using pizein plastic to provide a vacuum-tight seal. Using this adaptor, the quartz vessel was attached to a stainless-steel valve, which was then attached to a stainless-steel vacuum line. Afterwards, the quartz reaction vessel was flame dried 5 times using a Bunsen burner (propane gas). After adequate drying of the quartz vessel, 197.12 mg (0.56 mmol) $UF_6$ and 200.28 mg (0.95 mmol) $MoF_6$ (about a 1:1 wt mixture) were distilled into the quartz reaction vessel using liquid nitrogen cooling. The hexafluoride mixture was allowed to warm to room temperature to ensure adequate mixing. Afterwards, the hexafluoride mixture was cooled with liquid nitrogen and then 849 mbar (1.05 mmol) CO was added to the reaction vessel. The $UF_6/MoF_6/CO$ mixture was allowed to warm to room temperature. Afterwards, the mixture was irradiated with a 395 nm LED light for 24 h. After the first irradiation cycle, the mixture was cooled with liquid nitrogen and the $CO/COF_2$ mixture was pumped off under dynamic vacuum conditions. Another 853 mbar (1.05 mmol) CO was added to the reaction vessel. The mixture was then irradiated with a 395 nm LED light for another 24 h. After irradiation, the reaction mixture was cooled using liquid nitrogen and the $CO/CO_2$ was pumped off under dynamic vacuum conditions.

Once all $CO/CO_2$ had been pumped off, the $UF_5/MoF_6$ reaction mixture was allowed to warm and the $MoF_6$ was removed from the $UF_5$ sample via distillation to a 20 mL quartz vessel. This 20 mL quartz vessel was previously flame dried 5 times with a Bunsen burner. The $MoF_6$ sample was then cooled with liquid nitrogen and 913 mbar (7.96 mmol) CO were added to the vessel. The $MoF_6/CO$ mixture was irradiated with 395 nm light for 2 h. During this time, no pale green $UF_5$ had formed. Afterwards, the mixture was moved to a homemade UV reactor and irradiated with 254 nm light for 18 h in order to reduce the $MoF_6$ to $MoF_5$. The authors would also like to note that, if a larger quartz vessel was used, then this separation technique could be performed in a one-step process, i.e., “fresh” CO would not have to be added after a day of irradiation. In addition, with the use of a larger reaction vessel, and more than one 395 nm LED light, the time needed for the separation should significantly decrease.

Quantitative amounts of $UF_5$ and $MoF_6$ were obtained. The $UF_5$ was collected and stored in an PTFE vessel in an inert atmosphere glovebox. All further manipulation of this $UF_5$ sample was done in the same inert atmosphere glovebox. In order to perform elemental analyses on the $UF_5$ sample, the entire sample was ground using an agate mortar and pestle to ensure homogeneity (it was noticed that some hydrolysis occurred during this process, as the sample turned from pale green to grey green). Some of the $UF_5$ sample was subsequently transferred to three gelatin capsules. Capsule 1 contained 5.02 mg $UF_5$; Capsule 2 contained 5.42 mg $UF_5$; Capsule 3 contained 5.60 mg $UF_5$. The capsules were then dissolved in dilute nitric acid and microwaved to ensure complete dissolution. Finally, the dissolved samples were diluted with dilute nitric acid to 100 mL and analyzed by MP-AES. The remaining $UF_5$ sample was used for powder X-ray diffraction and IR spectroscopy.

In order to perform elemental analyses on the $MoF_5$ sample (produced by the reduction of the $MoF_6$ sample), the entire sample was dissolved in ca. 50 mL of distilled water. ***Cation: This dissolution process produces significant amounts of hydrogen fluoride. This procedure must be performed in a fume hood.*** Afterwards, 8 mL of concentrated (65 %) nitric acid was added to the sample and then the sample was diluted with distilled water to 100 mL. For analysis of this sample, 1 mL of the Mo solution was taken and further diluted to 25 mL using dilute nitric acid.

***Trial 2:*** Original amounts/first irradiation cycle: 204.42 mg (0.58 mmol) $UF_6$, 198.83 mg (0.95 mmol) $MoF_6$, and 847 mbar (1.04 mmol) CO. Second irradiation cycle: 845 mbar (1.04 mmol) CO. Quantitative yields of $UF_5$ and $MoF_6$ obtained. Amount of CO added to vessel containing $MoF_6$ (to reduce $MoF_6$ to $MoF_5$): 924 mbar (0.81 mmol). Amounts of $UF_5$ used for MP-AES analysis: Capsule 1 contained 5.49 mg of $UF_5$; Capsule 2 contained 4.94 mg of $UF_5$; Capsule 3 contained 5.16 mg of $UF_5$.

***Trial 3:*** Original amounts/first irradiation cycle: 206.86 mg (0.59 mmol) of $UF_6$, 198.83 mg (0.95 mmol) of $MoF_6$, and 845 mbar (1.04 mmol) of CO. Second irradiation cycle: 880 mbar (1.09 mmol) of CO. Quantitative yields of $UF_5$ and $MoF_6$ were obtained. Amount of CO added to the vessel containing $MoF_6$ (to reduce $MoF_6$ to $MoF_5$): 929 mbar (0.81 mmol). Amounts $UF_5$ used for MP-AES analysis: Capsule 1 contained 5.31 mg of $UF_5$; Capsule 2 contained 5.11 mg of $UF_5$; Capsule 3 contained 5.05 mg of $UF_5$.

***Trial 7:*** This trial was performed only to collect $MoF_5$ in order to obtain a powder X-ray diffraction pattern and IR spectrum. Instead of a quartz vessel, a 37 mL FEP reaction vessel was used for the separation reaction. A 36 mL FEP vessel was used for the reduction of $MoF_6$ to $MoF_5$. ***Note: FEP vessels are not recommended for these separation reactions because the hexafluorides are somewhat soluble in the plastic.*** Original amounts/first irradiation cycle: 172.68 mg (0.49 mmol) of $UF_6$, 161.04 mg (0.77 mmol) of $MoF_6$, and 1.03 bar (1.56 mmol) of CO. Second irradiation cycle: 1.03 bar (1.56 mmol) of CO. Quantitative yields of $UF_5$ and $MoF_6$ were obtained. Amount of CO added to vessel containing $MoF_6$ (to reduce $MoF_6$ to $MoF_5$): 1.03 bar (1.49 mmol).

### *4.3. Techniques and procedures for the separation of $MoF_6$ from $UF_6$ using sulfur dioxide and near UV light*

Because all trials that were performed to demonstrate the separation techniques are similar to each other, only Trial 4 will be discussed in detail here. For Trial 5 and Trial 6, only the amounts of starting materials, yields, and samples used for MP-AES analyses will be discussed.

***Trial 4:*** A 1-cm Teflon-coated stir bar was added to an approximately 30 mL homemade FEP reaction vessel. The vessel was then connected to a stainless-steel valve, and then to a metal vacuum line. The reaction vessel was placed under dynamic vacuum and then heated with a heat gun set to 120 °C for 2 h to ensure adequate dryness. Afterward, 201.99 mg (0.57 mmol) $UF_6$ and 197.38 (0.94 mmol) $MoF_6$ were distilled into the vessel using liquid nitrogen cooling. Onto the hexafluoride mixture, 7.53 mg (0.12 mol) $SO_2$ were condensed at −196 °C. The reaction mixture was warmed to room temperature and stirred using the stir bar and a stir plate. Once the hexafluorides were dissolved, the reaction mixture was irradiated with 395 nm light for 1 h and 30 min***. Note:*** Irradiation times seem to be dependent on the amount of $UF_6$ present. Larger samples of $UF_6$ may call for longer irradiation times. Afterwards, the $MoF_6/SO_2/SO_2F_2$ mixture was distilled into another 30 mL FEP vessel, which was previously dried through the procedure described above. This reaction mixture was warmed to room temperature and left for one week. After one week, the remaining $SO_2/SO_2F_2$ was pumped off under static vacuum and a white, crystalline sample of $MoOF_4$ remained in the FEP vessel.

The $UF_5$ and $MoOF_4$ samples were collected in an inert atmosphere glovebox and stored in PTFE containers. The yield of $UF_5$ was quantitative, whereas the yield of $MoOF_4$ was 72.00 %. To perform elemental analysis, the entire $UF_5$ sample or the entire $MoOF_4$ sample were ground using a agate mortar and pestle to ensure homogeneity. During this process, slight hydrolysis of both samples occurred, as noted by the color change (both samples turned somewhat greyish). For elemental analyses of $UF_5$, some of the sample was loaded into three gelatin capsules. Capsule 1 contained 2.64 mg of $UF_5$; Capsule 2 contained 2.47 mg of $UF_5$; Capsule 3 contained 2.59 mg of $UF_5$. For elemental analyses of the $MoOF_4$ sample, some of the sample was loaded into 3 gelatin capsules. Capsule 4 contained 2.58 mg of $MoOF_4$; Capsule 5 contained 2.65 mg of $MoOF_4$; Capsule 6 contained 3.08 mg of $MoOF_4$. All capsules were dissolved in dilute nitric acid and then microwaved to ensure dissolution. All samples were then diluted to 50 mL with dilute nitric acid for analysis by MP-AES. The remaining samples of $UF_5$ and $MoOF_4$ were used to obtain powder X-ray diffraction patterns and IR spectra.

***Trial 5:*** Starting amounts: 197.12 mg (0.56 mmol) of $UF_6$, 197.38 mg (0.94 mmol) of $MoF_6$, and 6.61 mg (0.10 mol) of $SO_2$. The yield of $UF_5$ was quantitative, whereas the yield of $MoOF_4$ was 60.42 %. Amount $UF_5$ used for elemental analyses: Capsule 1 contained 2.58 mg of $UF_5$; Capsule 2 contained 2.65 mg of $UF_5$; Capsule 3 contained 3.08 mg of $UF_5$. Amount $MoOF_4$ used for elemental analyses: Capsule 4 contained 5.15 mg of $MoOF_4$; Capsule 5 contained 5.22 mg of $MoOF_4$; Capsule 6 contained 6.24 mg of $MoOF_4$.

***Trial 6:*** Starting amounts: 201.99 mg (0.57 mmol) of $UF_6$, 198.83 mg (0.95 mmol) of $MoF_6$, and 6.75 mg (0.11 mol) of $SO_2$. The yield of $UF_5$ was quantitative, whereas the yield of $MoOF_4$ was 71.66 %. Amount $UF_5$ used for elemental analyses: Capsule 1 contained 3.28 mg of $UF_5$; Capsule 2 contained 2.77 mg of $UF_5$; Capsule 3 contained 2.56 mg of $UF_5$. Amount $MoOF_4$ used for elemental analyses: Capsule 4 contained 5.37 mg of $MoOF_4$; Capsule 5 contained 5.85 mg of $MoOF_4$; Capsule 6 contained 5.37 mg of $MoOF_4$.

### *4.4. Techniques and procedures for the separation of $MoF_6$ from $UF_6$ using supercritical carbon monoxide and near UV light*

The preparation and irradiation procedure was identical for both trials and was performed according to the previously given description. Both trials differed in the analytical treatment of the reaction products.

***Trial 1:*** Starting amounts: 44.58 (127 μmol) mg of $UF_6$, 17.99 mg (86 μmol) of $MoF_6$, and 42 bar (6.5 mmol) of CO. At end of irradiation, the cold finger of high-pressure container was cooled to −69 °C in order to maintain $MoF_6$ and unreacted $UF_6$ in the solid phase. The volatile species were removed at this temperature from the high-pressure container and analyzed using IR spectroscopy. The pressure in the measuring cell was 1.7 bar.

***Trial 2:*** Starting amounts: 39.70 mg (112 μmol) of $UF_6$, 16.43 mg (78 μmol) of $MoF_6$, and 56 bar (8.7 mmol) of CO. At end of irradiation, the high-pressure container was not cooled, but instead all components that were volatile at room temperature were condensed into a passivated stainless steel AISI 316 L storage container using liquid nitrogen. The volatiles were pumped off at this temperature. The storage container was allowed to warm to room temperature and its contents were again sublimed into a dried FEP vessel using liquid nitrogen. The vessel was vented under constant cooling, water was added and finally the liquid nitrogen was removed, allowing the vessel to warm to room temperature. MP-AES was performed on the resulting solution. The double transfer was performed in order to avoid a potential overloading of the FEP vessel by a rapid decompression of the high-pressure container. The high-pressure container was emptied at room temperature under an argon atmosphere and the extracted residues were dissolved in 50/50 (V/V) water/conc. $HNO_3$ and the solution also analyzed by MP-AES. Small amounts of the residues were lost, because they adhered to the FFKM O-ring and remained in difficult to reach regions of the high-pressure container.

### *4.5. Powder X-ray diffraction*

Powder X-ray diffraction patterns were obtained with a Stadi-MP-Diffractometer (STOE) using Cu-Kα radiation (λ =1.54051 Å), a germanium monochromator, and a Mythen1K detector. The data were handled using the WINXPOW software [36]. The compounds were filled into borosilicate capillaries, which were previously flamed dried under vacuum, and sealed using a hot tungsten wire under inert atmosphere in a glovebox.

### *4.6. Infrared spectroscopy*

The IR spectra were measured on an alpha FTIR spectrometer (Bruker) using a diamond ATR unit under an Ar atmosphere. The spectrum was processed with the OPUS software package [37]. Gas phase IR was measured in a specially designed and passivated measuring cell manufactured from stainless steel AISI 316 L, equipped with $BaF_2$ single crystal windows.

### *4.7. Microwave plasma atomic emission spectroscopy*

The quantification of the elements was done by microwave plasma atomic emission spectroscopy using a 4200 MP-AES spectrometer (Agilent). Nitrogen was used for plasma generation. Samples were solubilized using 8 mL concentrated $HNO_3$ within 100 mL of solution, or with 4 mL concentrated $HNO_3$ within 50 mL of solution. Commercial uranium and molybdenum standard solutions were used for calibration of the instrument.

## Declaration of Competing Interest

The authors report no declarations of interest.

## Acknowledgments

We thank Dr. Uwe Linne, Marburg, and his team for aid with the U and Mo analyses.

## Appendix A. Supplementary data

Supplementary material related to this article can be found, in the online version, at doi:https://doi.org/10.1016/j.jfluchem.2020.109655.

## References

[1] Nuclear and Radiation Studies Board, Division on Earth and Life Studies, National Academies of Sciences, Engineering, and Medicine, in: Opportunities and Approaches for Supplying Molybdenum-99 and Associated Medical Isotopes to Global Markets: Proceedings of a Symposium, National Academies Press, Washington, D.C., 2018, https://doi.org/10.17226/24909.

[2] OECD, Nuclear Energy Agency, The Supply of Medical Isotopes: An Economic Diagnosis and Possible Solutions, OECD, 2019, https://doi.org/10.1787/9b326195-en.

[3] Committee on State of Molybdenum-99 Production and Utilization and Progress Toward Eliminating Use of Highly Enriched Uranium, Nuclear and Radiation Studies Board, Division on Earth and Life Studies, National Academies of Sciences, Engineering, and Medicine, Molybdenum-99 for Medical Imaging, National Academies Press, Washington, D.C, 2016, https://doi.org/10.17226/23563.

[4] C. Green, Technetium-99m production issues in the United Kingdom, J. Med. Phys. 37 (2012) 66, https://doi.org/10.4103/0971-6203.94740.

[5] The Hague Nuclear Security Summit Communique, 2014.

[6] The Washington Nuclear Security Summit Communique, 2016.

[7] NEA/SEN/HLGMR, Market Impacts of Converting to Low-enriched Uranium Targets for Medical Isotope Production, 2012.

[8] S. Dittrich, History and actual state of non-HEU fission-based Mo-99 production with low-performance research reactors, Sci. Technol. Nucl. Install. 2013 (2013) 1–9, https://doi.org/10.1155/2013/514894.

[9] S.A. Ali, H.J. Ache, Production techniques of fission Molybdenum-99, Radiochim. Acta 41 (1987), https://doi.org/10.1524/ract.1987.41.23.65.

[10] S.-K. Lee, G.J. Beyer, J.S. Lee, Development of industrial-scale fission 99Mo production process using low enriched uranium target, Nucl. Eng. Technol. 48 (2016) 613–623, https://doi.org/10.1016/j.net.2016.04.006.

[11] T. Hollmer, W. Petry, A novel monolithic LEU foil target based on a PVD manufacturing process for 99Mo production via fission, Appl. Radiat. Isot. 118 (2016) 290–296, https://doi.org/10.1016/j.apradiso.2016.10.003.

[12] J.V. Beitz, C.W. Williams, Photochemical Removal of NpF6 and PuF6 from UF6 Gas Streams, 1990.

[13] J.V. Beitz, Removal of Fluoride Impurities from UF6 Gas, US4555318, 1985.

[14] Mark Fields, Metal Fluorides Separation, WO 97/38785, 1997.

[15] G.W. Halstead, P.G. Eller, L.B. Asprey, K.V. Salazar, Convenient multigram syntheses of uranium pentafluoride and uranium pentaethoxide, Inorg. Chem. 17 (1978) 2967–2969, https://doi.org/10.1021/ic50188a059.

[16] J.R. Geichman, E.A. Smith, S.S. Trond, P.R. Ogle, Hexafluorides of molybdenum, tungsten, and uranium. I. Reactions with nitrous and nitric oxides, Inorg. Chem. 1 (1962) 661–665, https://doi.org/10.1021/ic50003a042.

[17] H.J. Hurst, P.W. Wilson, The electronic absorption Spectrum of gaseous uranium hexachloride and hexafluoride, Spectrosc. Lett. 5 (1972) 275–279, https://doi.org/10.1080/00387017208064964.

[18] K.N. Tanner, A.B.F. Duncan, Raman effect and ultraviolet absorption spectra of molybdenum and tungsten hexafluorides[1], J. Am. Chem. Soc. 73 (1951) 1164–1167, https://doi.org/10.1021/ja01147a085.

[19] T.J. Ouellette, C.T. Ratcliffe, D.W.A. Sharp, Vibrational spectra of molybdenum and tungsten pentafluorides, J. Chem. Soc. A (1969) 2351, https://doi.org/10.1039/j19690002351.

[20] W.H. Zachariasen, Crystal chemical studies of the 5 *f* -series of elements. XI. The crystal structure of α-UF $_5$ and of β-$UF_5$, Acta Cryst. 2 (1949) 296–298, https://doi.org/10.1107/S0365110X4900076X.

[21] E. Jacob, Beiträge zur Chemie der Uranfluoride und -oxidfluoride. II. Darstellung und Schwingungsspektren von? - und? -Uranpentafluorid, Z, Anorg. Allg. Chem. 400 (1973) 45–50, https://doi.org/10.1002/zaac.19734000107.

[22] R.E. Stene, B. Scheibe, C. Pietzonka, A.J. Karttunen, W. Petry, F. Kraus, MoF 5 revisited. A comprehensive study of MoF 5, J. Fluorine Chem. 211 (2018) 171–179, https://doi.org/10.1016/j.jfluchem.2018.05.002.

[23] N. Acquista, S. Abramowitz, Vibrational spectrum of MoF5, J. Chem. Phys. 58 (1973) 5484–5488, https://doi.org/10.1063/1.1679170.

[24] A.J. Edwards, B.R. Steventon, Fluoride crystal structures. Part II. Molybdenum oxide tetrafluoride, J. Chem. Soc. A (1968) 2503, https://doi.org/10.1039/j19680002503.

[25] A. Lee Smith, The Coblentz Society Desk Book of Infrared Spectra, 2nd ed., The Coblentz Society, 1977.

[26] J.L. Hencher, G.W. King, Oxalyl halides, J. Mol. Spectrosc. 16 (1965) 168–178, https://doi.org/10.1016/0022-2852(65)90095-0.

[27] T.G. Burke, D.F. Smith, A.H. Nielsen, The molecular structure of MoF $_6$, WF $_6$, and UF $_6$ from infrared and Raman spectra, J. Chem. Phys. 20 (1952) 447–454, https://doi.org/10.1063/1.1700440.

[28] R.S. McDowell, R.J. Sherman, L.B. Asprey, R.C. Kennedy, Vibrational spectrum and force field of molybdenum hexafluoride, J. Chem. Phys. 62 (1975) 3974–3978, https://doi.org/10.1063/1.430320.

[29] A. Michels, T. Wassenaar, Th.N. Zwietering, The vapour pressure of carbon monoxide, Physica 18 (1952) 160–162, https://doi.org/10.1016/S0031-8914(52)80018-7.

[30] J. Stoll, J. Vrabec, H. Hasse, A set of molecular models for carbon monoxide and halogenated hydrocarbons, J. Chem. Phys. 119 (2003) 11396–11407, https://doi.org/10.1063/1.1623475.

[31] T. Shinoda, Vapor pressure of carbon monoxide in condensed phases, Bull. Chem. Soc. Jpn. 42 (1969) 2815–2820, https://doi.org/10.1246/bcsj.42.2815.

[32] R.P. Pohanish, Sittigs Handbook of Toxic and Hazardous Chemicals and Carcinogens, 7th ed., Elsevier, 2017.

[33] A.J. Edwards, R.D. Peacock, R.W.H. Small, 868. The preparation and structure of molybdenum pentafluoride, J. Chem. Soc. (1962) 4486–4491, https://doi.org/10.1039/JR9620004486.

[34] P.G. Eller, A.C. Larson, Crystal structures of alpha-UF5 and U2F9 and spectral characterization of U2F9, Inorg. Chim. Acta 37 (1979) 129–133.

[35] R.R. Ryan, R.A. Penneman, L.B. Asprey, R.T. Paine, Single-crystal X-ray study of β-uranium pentafluoride. The eight coordination of U(V), Acta Crystallogr. B 32 (1976) 3311–3313, https://doi.org/10.1107/S0567740876010182.

[36] STOE WinXPOW, STOE & Cie GmbH, Darmstadt, Germany, 2015.

[37] OPUS, Bruker Optik GmbH, Ettlingen, Germany, 2009.